



**Fermi National Accelerator Laboratory**

TM -1922

**Lattice Function Measurement with TBT BPM Data<sup>†</sup>**

Ming-Jen Yang

Fermi National Accelerator Laboratory

P.O. Box 500, Batavia, Illinois

March 1995

---

<sup>†</sup> To be submitted at the 1995 IEEE Particle Accelerator Conference, Dallas, Texas, May 1-5, 1995.

 Operated by Universities Research Association, Inc., under contract with the United States Department of Energy.

1.	Introduction .....	2
2.	Basics and formula of TBT analysis .....	4
2.1	What's different about the TBT method .....	4
2.2	Machine criteria for TBT data .....	4
2.2.1	Chromoticity .....	4
2.2.2	Coupling .....	5
2.2.3	Betatron oscillation amplitude .....	5
2.2.4	Beam loss .....	5
2.3	Fitting for phase space parameters .....	5
2.4	Ellipse and lattice function .....	6
2.5	Tune .....	8
2.6	Coupling measurement .....	8
2.6.1	Global coupling .....	8
2.6.2	Local coupling .....	8
3.	TBT system .....	10
3.1	Hardware .....	10
3.2	Data acquisition .....	10
3.4	Software support .....	10
4.	Analysis .....	11
4.1	Data pre-processing .....	11
4.2	Fitting for beam parameters .....	11
4.2.1	Fit deviation statistics .....	11
4.2.2	Diagnostics .....	13
4.2.3	TBT $Dp/p$ .....	14
4.2.4	Lattice verification .....	15
4.3	Fitting the phase space ellipse .....	15
4.3.1	Lattice function calculation .....	16

4.3.2	Tune .....	17
4.3.3	Error estimate .....	18
5.	Simulation .....	21
5.1	Noise and data resolution .....	21
5.2	Transfer matrix .....	22
5.3	Lattice function error .....	24
6.	Conclusion .....	26

Figure 1,	The Layout of BPM's in the D3 & D4 section.....	2
Figure 2.	The horizontal BPM position .....	2
Figure 3.	The phase space plot.....	3
Figure 5.	The BPM deviation statistics .....	12
Figure 6.	BPM deviation.....	13
Figure 7.	Histogram of BPM HPD32 deviation.....	14
Figure 8.	The refitted TBT RMS deviation .....	14
Figure 9.	The $\Delta P/P$ plot.....	15
Figure 10.	X and X' phase space plot.....	16
Figure 11.	The lattice function at the BPM locations.....	17
Figure 12.	The normalized phase space plot .....	17
Figure 13.	TBT tune calculation .....	18
Figure 14.	Histogram of fitted beta function .....	19
Figure 15.	The fitted beta plotted against the turn number .....	20
Figure 16.	BPM position deviation using simulated data .....	21
Figure 17.	The BPM position deviation with simulation error .....	22
Figure 18,	FFT spectrum from the simulated data.....	23
Figure 19.	The FFT spectrum from actual data .....	24
Figure 20.	The deviation RMS of fitted beta .....	24
Figure 21.	The RMS of fitted beta value distribution.....	25

# Lattice Function Measurement with TBT BPM Data

Ming-Jen Yang

Fermi National Accelerator Laboratory

## Abstract

At Fermilab Main Ring some of the Beam Position Monitors (BPM) are instrumented with Turn-By-Turn (TBT) capability to record up to 1024 consecutive turns of BPM data for each given trigger. For example, there are 9 horizontal plane and 8 vertical plane BPM's in the sector D3 & D4. The BPM data, which records the betatron oscillation, is fitted to obtain beam parameters  $x$ ,  $x'$ ,  $y$ ,  $y'$ , and  $\Delta p/p$ , using the calculated beam line transfer matrix. The resulted TBT beam parameters ( $x$ ,  $x'$ ) or ( $y$ ,  $y'$ ) are fitted to ellipses to obtain the lattice function  $\beta$ ,  $\alpha$ , and the emittance associated with the betatron oscillation. The tune of the machine can be calculated from the phase space angles of the successive turns, in the normalized phase space. The beam parameters can also be used to extract transfer matrix to be used for local and global coupling analysis. The process of fitting the BPM data produces information that can be used to diagnose problems such as calibration, noise level and polarity. Being available at every turn and at changing beam position the information carries a lot of statistical power. Since most of the BPM's are located at high beta location only the  $x$  and  $y$  beam position information is not simultaneously available. The BPM data fitting processing essentially bridged the gap.

## 1. Introduction

Single BPM Turn-by-Turn beam position data in a circular machine is usually used to do tune measurement with the FFT analysis. With multiple BPM turn-by-turn data there are more possibilities.

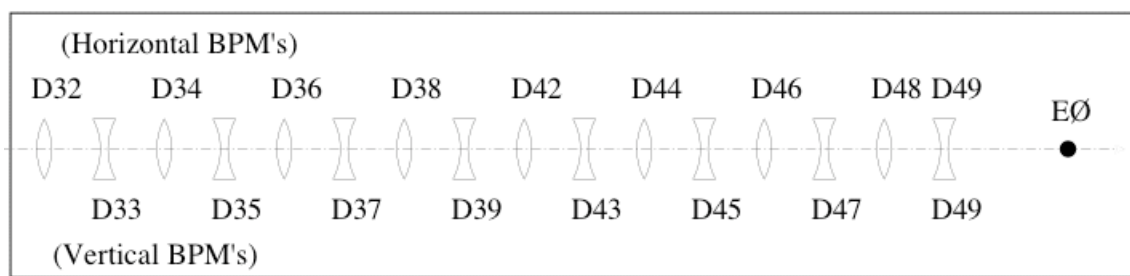


Figure 1, The Layout of BPM's in the D3 & D4 section of the D-sector of Fermilab Main Ring. The horizontal BPM's are listed on the top side of the figure and the vertical BPM's on the bottom side. The EØ location has no BPM instrumentation but is where the fitting for  $x$  and  $x'$  is referenced to.

At Fermilab one way of measuring lattice function has been developed using TBT betatron oscillation data. Figure 1 shows all the BPM's in the Fermilab Main Ring sector D3 & D4, in either plane. Using the known transfer matrix from one BPM to another the position data can be fitted to get beam parameters  $x$  and  $x'$  for a given reference location for every turn of the beam. In this example the reference location was chosen to be at the EØ straight which is down stream of M:HPD49. In Figure 2 shows a single turn BPM data in open circles. The expected BPM position after the fit is shown in solid dots.

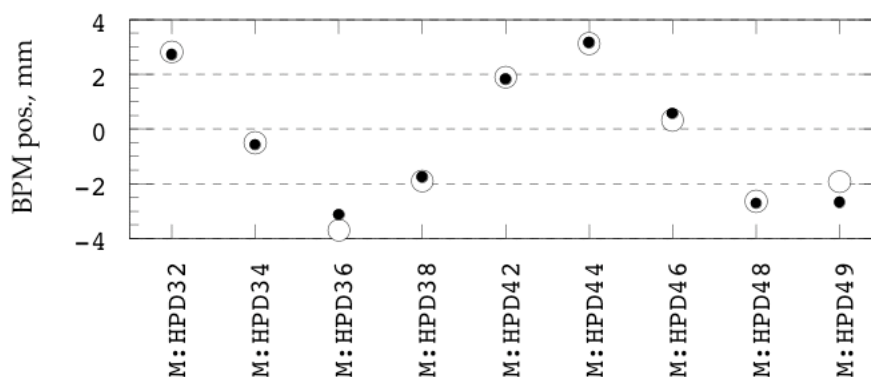


Figure 2. The horizontal BPM position is plotted for each BPM in the beam line. The open circles are the actual BPM data and the solid dots are the calculated beam positions based on the fitted  $x$  and  $x'$  at EØ.

The resulting EØ location beam phase space parameters  $x$  and  $x'$  are plotted in Figure 3, which includes a total of 200 consecutive turns. These points, which follow elliptical path as dictated by the tune and the lattice function of the machine, are fitted to an ellipse to extract  $\beta$  and  $\alpha$  function. With the fitted lattice function the tune of the machine can be calculated using the normalized phase space angle, in a turn-by-turn fashion.

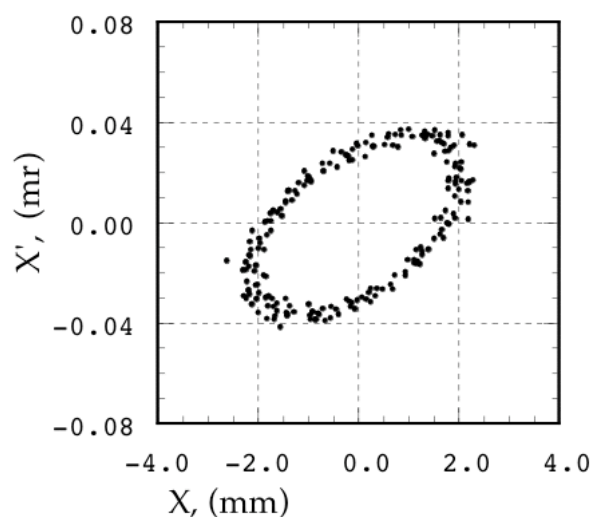


Figure 3. The phase space plot of fitted beam parameters ( $x$ ,  $x'$ ) at EØ. Each point represents one turn of the proton beam. There are a total of 200 consecutive turns on the plot.

In this write-up the whole mechanism of the TBT analysis will be presented fully. Also included are the mathematics, the TBT system hardware and software, the analysis of a set of actual TBT data, and the analysis of simulated TBT data as well.

## 2. Basics and formula of TBT analysis

### 2.1 WHAT'S DIFFERENT ABOUT THE TBT METHOD

The beta function can be measured by using either dipole or quadrupole correctors. Since the number of independently adjustable quadrupoles are very limited at Fermilab Main Ring the one-bump dipole method is by far the most used. This method uses closed orbit changes as a function of calibrated kicks from dipole corrector [1] to calculate the beta function. The TBT method uses the betatron oscillation data to extract lattice function.

The one-bump method needs the phase advances between BPM's or around the ring called the tune. The TBT method needs the beam line transfer matrix in between the BPM's. These information about the machine are basically equivalent but in a different form. In other word both have to start with a model of some kind.

There are some important differences between the two methods. First, the one-bump method needs phase advance covering all devices in the ring while the TBT method needs transfer matrix only between the BPM's. In other words, one needs a global information while the other only needs local information. Second, The TBT method has some self diagnosing information while the one-bump method does not. A wrong transfer matrix used in the TBT method will result in a poor fit. Third, the one-bump method needs the calibrations of the corrector dipole strength while the TBT method does not care how the betatron oscillation is excited.

### 2.2 MACHINE CRITERIA FOR TBT DATA

Since the betatron oscillation is the soul of TBT lattice function measurement it is very important to keep its amplitude steady. The effects which degrade TBT data quality should be avoided.

#### 2.2.1 Chromoticity

The observed betatron amplitude changes its amplitude through process of decoherence, which depends on both  $\Delta p/p$  and chromoticity  $\xi$ . The  $\Delta p/p$  is usually not some thing that gets changed easily. The chromoticity on the other



hand is usually kept at non-zero value due to instability. However, it can be set to nearly zero for a shot time or with smaller intensity beam during study. It is important that changing  $\xi$  does not significantly change the machine. Monitoring the tune of the machine will give indication of possible sextupole feed-down effect.

### 2.2.2 Coupling

Another way the betatron oscillation can change its amplitude very quickly is through X-Y coupling. In this case the betatron amplitude is modulated by the beat frequency caused by the oscillation in the two planes. It is essential that the machine be sufficiently de-coupled by either the use of correctional skew quadrupole or by pulling the tunes of the two planes apart. Having a zero chromaticity in both planes can make things more complicated if coupling is not reduced sufficiently.

### 2.2.3 Betatron oscillation amplitude

The amplitude of the betatron oscillation should be large enough that the noise level does not cause significant error.

### 2.2.4 Beam loss

When the betatron oscillation amplitude becomes too large some portion of the beam may be outside of the dynamic aperture and be loss. If sufficient amount of beam is lost in a short time the beam position may not be reliable.

## 2.3 FITTING FOR PHASE SPACE PARAMETERS

In the horizontal plane the BPM data of each single turn is fitted for the beam parameter  $x$ ,  $x'$ , and  $\Delta p/p$  at a reference beam line location. The vertical plane TBT data is fitted only for  $y$  and  $y'$ . The beam line transfer matrix between this reference zero-th location and the  $i$ -th BPM locations is shown in the following equation:

$$\begin{pmatrix} x_i \\ x_i' \\ \delta \end{pmatrix} = \begin{bmatrix} T_{11}^i & T_{12}^i & T_{13}^i \\ T_{21}^i & T_{22}^i & T_{23}^i \\ 0 & 0 & 1 \end{bmatrix} \cdot \begin{pmatrix} x_o \\ x_o' \\ \delta \end{pmatrix} \quad (1)$$

$\delta$  ( $= \Delta p/p$ ) is the percentage deviation of the average beam momentum from the reference momentum as determined by the bending field. The inclusion of  $\delta$  in

the calculation is necessary to remove the effect of momentum error. The  $x_o$ ,  $x_o'$ , and  $\delta$  of the column vector on the right hand side are the beam parameters being fitted to the reference o-th location. This fit is done by minimizing the summed quantity below:

$$S = \sum_i (p_i - x_i)^2 = \sum_i (p_i - x_o \cdot T_{11}^i - x_o' \cdot T_{12}^i - \delta \cdot T_{13}^i)^2 \quad (2)$$

The summing index "i" is for all the BPM's being used for the calculation. " $p_i$ " is the i-th BPM reading. Taking the partial derivatives of S with respect to the beam parameters gives:

$$\begin{aligned} \frac{\partial S}{\partial x_o} &= \sum_i (p_i - x_o \cdot T_{11}^i - x_o' \cdot T_{12}^i - \delta \cdot T_{13}^i) \cdot T_{11}^i = 0 \\ \frac{\partial S}{\partial x_o'} &= \sum_i (p_i - x_o \cdot T_{11}^i - x_o' \cdot T_{12}^i - \delta \cdot T_{13}^i) \cdot T_{12}^i = 0 \\ \frac{\partial S}{\partial \delta} &= \sum_i (p_i - x_o \cdot T_{11}^i - x_o' \cdot T_{12}^i - \delta \cdot T_{13}^i) \cdot T_{13}^i = 0 \end{aligned}$$

After completing all the summed terms one obtains:

$$\Rightarrow \begin{pmatrix} U_1 \\ U_2 \\ U_3 \end{pmatrix} = \begin{bmatrix} R_{11} & R_{12} & R_{13} \\ R_{21} & R_{22} & R_{23} \\ R_{31} & R_{32} & R_{33} \end{bmatrix} \cdot \begin{pmatrix} x_o \\ x_o' \\ \delta \end{pmatrix} \quad (3)$$

The  $3 \times 3$  matrix R depends only on the T matrix elements. The  $U$  column vector on the other hand depends also on the measured BPM position data. From equation (3) the beam parameters is solved. The result can then be propagated to other BPM location using equation (1). This procedure is to be done for every single turn of the BPM data.

## 2.4 ELLIPSE AND LATTICE FUNCTION

A parameter representation of a phase space ellipse can be written as follows [2]:

$$\begin{pmatrix} x_n \\ x_n' \end{pmatrix} = \begin{pmatrix} \sqrt{\beta} \cdot \sqrt{\epsilon} \cdot \cos(\phi_n - \phi_o) \\ -(\sqrt{\epsilon}/\sqrt{\beta}) \cdot [\sin(\phi_n - \phi_o) + \alpha \cdot \cos(\phi_n - \phi_o)] \end{pmatrix} \quad (4)$$

The  $x_n$  and  $x_n'$  are the phase space coordinate at the n-th turn. This expression is useful for plotting the ellipse with given  $\epsilon$ ,  $\beta$ , and  $\alpha$ . The emittance  $\epsilon$  here is simply the phase space area enclosed by the ellipse.

To fit for  $\alpha$ ,  $\beta$ , and  $\varepsilon$  with a given series of phase space points a different formula is used. Start with the normalized phase space coordinate transformation:

$$\begin{pmatrix} X_n \\ Y_n \end{pmatrix} = \begin{pmatrix} x_n / \sqrt{\beta} \\ \sqrt{\beta} \cdot x_n' + \alpha \cdot x_n / \sqrt{\beta} \end{pmatrix}. \quad (5)$$

The phase space point  $(X_n, Y_n)$  will follow a circular path. Re-scale this coordinate space with the factor  $\frac{1}{\sqrt{\beta}}$  to get.

$$\begin{pmatrix} U_n \\ V_n \end{pmatrix} = \frac{1}{\sqrt{\beta}} \cdot \begin{pmatrix} X_n \\ Y_n \end{pmatrix} = \begin{pmatrix} x_n / \beta \\ x_n' + (\alpha/\beta) \cdot x_n \end{pmatrix} = \begin{pmatrix} a \cdot x_n \\ x_n' + b \cdot x_n \end{pmatrix}, \quad (6)$$

where  $a = \frac{1}{\beta}$  and  $b = \frac{\alpha}{\beta}$ . The trajectory in the  $(U, V)$  phase space is still expected to be circular. Using equation (6) as transformation to the  $(U, V)$  phase space points and fit for the best circular path by minimizing the equation of deviation from circular trajectory

$$S = \sum_n [R^2 - (a \cdot x_n)^2 - (x_n' + b \cdot x_n)^2]^2. \quad (7)$$

The summation over  $n$  is for the number of turns used in the phase space ellipse. With a little massage and substitution of  $A = -(a^2 + b^2)$ ,  $B = -2b$  and  $C = R^2$  the equation becomes

$$S = \sum_n [A \cdot x_n^2 + B \cdot x_n \cdot x_n' + C - x_n'^2]^2. \quad (8)$$

Taking the partial derivatives w.r.t.  $S$  gives the three simultaneous equations for solving  $A$ ,  $B$ ,  $C$ :

$$\begin{aligned} \frac{\partial S}{\partial A} &= \sum_n [A \cdot x_n^2 + B \cdot x_n \cdot x_n' + C - x_n'^2] \cdot x_n^2 = 0 \\ \frac{\partial S}{\partial B} &= \sum_n [A \cdot x_n^2 + B \cdot x_n \cdot x_n' + C - x_n'^2] \cdot x_n \cdot x_n' = 0 \\ \frac{\partial S}{\partial C} &= \sum_n [A \cdot x_n^2 + B \cdot x_n \cdot x_n' + C - x_n'^2] = 0 \end{aligned}$$

Once the equations are solved the value for  $\alpha$ ,  $\beta$ , and  $\varepsilon$  can be calculated with the formula of substitution defined. The  $\varepsilon$  value simply is the area enclosed by the ellipse which means  $\varepsilon = \beta \cdot R^2$ , in unit of  $\pi$ -mm-mr.

## 2.5 TUNE

With the normalized phase space transformation of equation (5) one can calculate the phase space angle

$$\theta_n = \tan^{-1}[X_n, Y_n] + \Delta\Phi_n \quad (9)$$

and the TBT tune is simply

$$\nu_n = \theta_n - \theta_{n-1}. \quad (10)$$

$\Delta\Phi_n$  is an adjustment in increment of  $2\pi$  such that  $\nu_n$  does not change sign. Because of data precision the TBT tune will not be noise free. A more precise number can be obtained by doing linear fit to  $\theta_n$  against the turn number. The slope from the fit gives the tune of the machine.

## 2.6 COUPLING MEASUREMENT

### 2.6.1 Global coupling

The equation for global coupling is expressed as

$$\begin{pmatrix} x \\ x' \\ y \\ y' \end{pmatrix}^{(n+1)} = \begin{bmatrix} M_{11} & M_{12} & M_{13} & M_{14} \\ M_{21} & M_{22} & M_{23} & M_{24} \\ M_{31} & M_{32} & M_{33} & M_{34} \\ M_{41} & M_{42} & M_{43} & M_{44} \end{bmatrix} \begin{pmatrix} x \\ x' \\ y \\ y' \end{pmatrix}^{(n)}. \quad (11)$$

The superscript of the column vector is used to indicate the turn number. Since the column vectors are calculated independently for each turn the whole ring transfer matrix elements can be fitted by minimizing the expression in equation (12).

$$S_j = \sum_n [u_j^{n+1} - \sum_{i=1}^4 M_{ji} \cdot u_i^n]^2 \quad (12)$$

The row index  $j$  is used because the matrix elements are fitted row by row. The  $u_j$  are defined as the  $j$ -th row of the column vector.

### 2.6.2 Local coupling

The equation for local coupling is expressed as

$$\begin{pmatrix} x \\ x' \\ y \\ y' \end{pmatrix}_+^{(n)} = \begin{bmatrix} M_{11} & M_{12} & M_{13} & M_{14} \\ M_{21} & M_{22} & M_{23} & M_{24} \\ M_{31} & M_{32} & M_{33} & M_{34} \\ M_{41} & M_{42} & M_{43} & M_{44} \end{bmatrix} \cdot \begin{pmatrix} x \\ x' \\ y \\ y' \end{pmatrix}_-^{(n)}. \quad (13)$$

The subscript "+" or "-" are used to indicate if the beam vector is calculated using the down-stream or up-stream TBT BPM data. The superscript again indicates the n-th turn data. The formula for fitting local coupling transfer matrix is slightly different from that of the global coupling and is shown in equation (14).

$$S_j = \sum_n [u_{j+}^n - \sum_{i=1}^4 M_{ji} \cdot u_{i-}^n]^2 \quad (14)$$

To do the local coupling calculation properly it is of course important to have sufficient number of BPM detectors on either side of the location where analysis is to be done.

### 3. TBT system

#### **3.1 HARDWARE**

At Fermilab both Tevatron and Main Ring use the same BPM hardware. There are 24 multi-bus based BPM houses around the ring [3]. Each house handles up to 6 horizontal and 6 vertical BPM's. The TBT hardware is simply a multi-bus TBT memory card with a data storage space of  $1024 \times 14$  bytes. This space is for 12 one-byte BPM data and a two-byte TBT time stamp for 1024 turns. Two timing signals are used to prepare for and to trigger the TBT data collection. All micro-processors are already programmed to handle the TBT data.

Currently A1 & A2 and D3 & D4 houses in the Main Ring are instrumented with TBT hardware. The TBT data from A1 & A2 location is useful for studying the Main Ring injection matching from 8 GeV line and the data from D3 & D4 houses for extraction matching to Tevatron. In Tevatron the E1 & E2 BPM houses are instrumented with TBT hardware and can be used to study the beam injection from the Main Ring. The Tevatron A4 & B1 houses are recently instrumented with the hope to study the beta function at the BØ collision point.

#### **3.2 DATA ACQUISITION**

Both the Main Ring and Tevatron BPM data request are serviced by the Tevatron front end. The front end and the multi-bus processor communicates using the GAS protocol via CAMAC data way. In the past the demand for TBT data has always been one horizontal and one vertical only, as was requested by the application program. With the new demand there is now two BPM houses worth of data, approximately 24 Kilo-Bytes, to be read.

#### **3.4 SOFTWARE SUPPORT**

Console program M42 was originally written to do only the FFT analysis on the TBT data. It is upgraded to do just about every thing being covered in this write-up and more. There is help facility on the new M42 console program (W42) to give a description of the new functionality.

## 4. Analysis

### 4.1 DATA PRE-PROCESSING

Before analysis could begin the closed-orbit is subtracted from each BPM data. For each BPM the closed-orbit is simply the average position over the number of turns sampled. The BPM positions shown in figure 2 already had the closed orbit subtracted. Otherwise the regular sine-wave like betatron oscillation would have been obscured by the irregular orbit offsets. When significant synchrotron oscillation is present at a period comparable to the duration of data sample more care must be taken to avoid introducing bias.

### 4.2 FITTING FOR BEAM PARAMETERS

The fitting procedure follows the formula as outlined in section 2.2. With the fitted result the expected position at every BPM can be calculated and be compared with data. It is important that the fit deviations at all the BPM's are checked to ensure the validity of result. A statistical analysis usually can provide a quick glance at the deviation error and show if potential problem is present. This deviation can always be examined as is to see if any systematic error is hidden behind the statistics. It is always a good idea to look at the deviation data itself to see if there exist systematic effects.

#### 4.2.1 Fit deviation statistics

The deviation statistics is collected and examined in two ways. The first, called "TBT RMS error," is to collect it across all the BPM's and compare it from one turn to another. The other way, called "BPM error", is to collect the statistics on individual PBM over a range of turn number and compare that with other BPM.

##### 4.2.1.1 TBT RMS error

After the fit the Root-Mean-Square deviation of equation (2) is evaluated for every turn. The TBT RMS error is expected to be independent of the turn number and be consistent with the expected RMS due to BPM electronics noise and the digitization resolution. By comparing it turn by turn problems with data

may be identified. As an example, Figure 4 shows the TBT RMS as a function of turns.

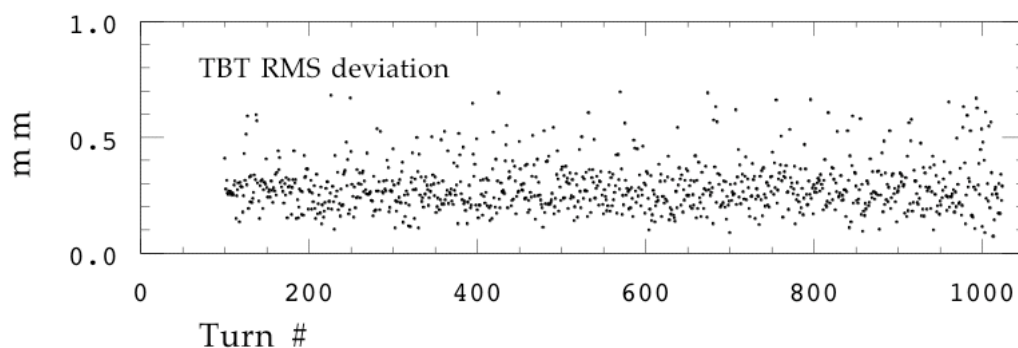


Figure 4. Turn-by-turn Root-Mean-Square deviation of BPM data from the fitted result.

There could be various indication for error. A sudden huge jump in RMS is likely caused by one of the two BPM houses skipping a couple of turns resulting in data from the two BPM houses not matching in time. A RMS which tends to follow the betatron amplitude may be an indication that the transfer matrix used is incorrect.

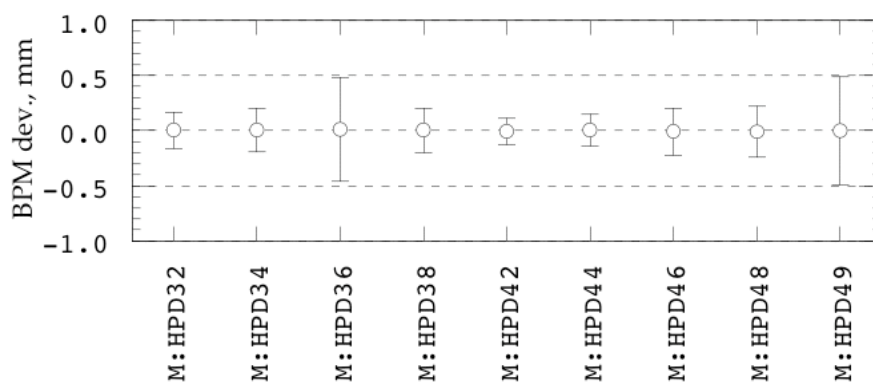


Figure 5. The BPM deviation statistics. This is based on individual BPM can be collected for any number of turns. Shown in this plot is data accumulated from about 200 turns. The open circle represent the average of deviations and error bar is the RMS of the deviation.

#### 4.2.1.2 BPM error

The average and RMS deviation between data and the fit can be collected for individual BPM at any number of turns. The result is shown in Figure 5, from the same data set. The average of position deviation, shown in open circles, is expected to be nearly zero and would indicate problems if otherwise. The



RMS, shown as the vertical error bars, is a useful indicator of individual BPM problems such as noise, poor calibrations, or even wrong signal polarity.

#### 4.2.2 Diagnostics

While the RMS error shown in Figure 4 seemed a bit noisy the BPM error in Figure 5 says that both HPD36 and HPD49 have significantly larger RMS in their errors. A plot of their turn-by-turn deviation and that of HPD32 is shown in Figure 6. The histogram of HPD32 deviation shown in Figure 7 is roughly Gaussian and centered around zero, as expected for a normal BPM. This is not the case for the other two BPM's. By removing these two noisy ones from the fit the TBT RMS deviation improvement can be seen by comparing Figure 8 with Figure 4.

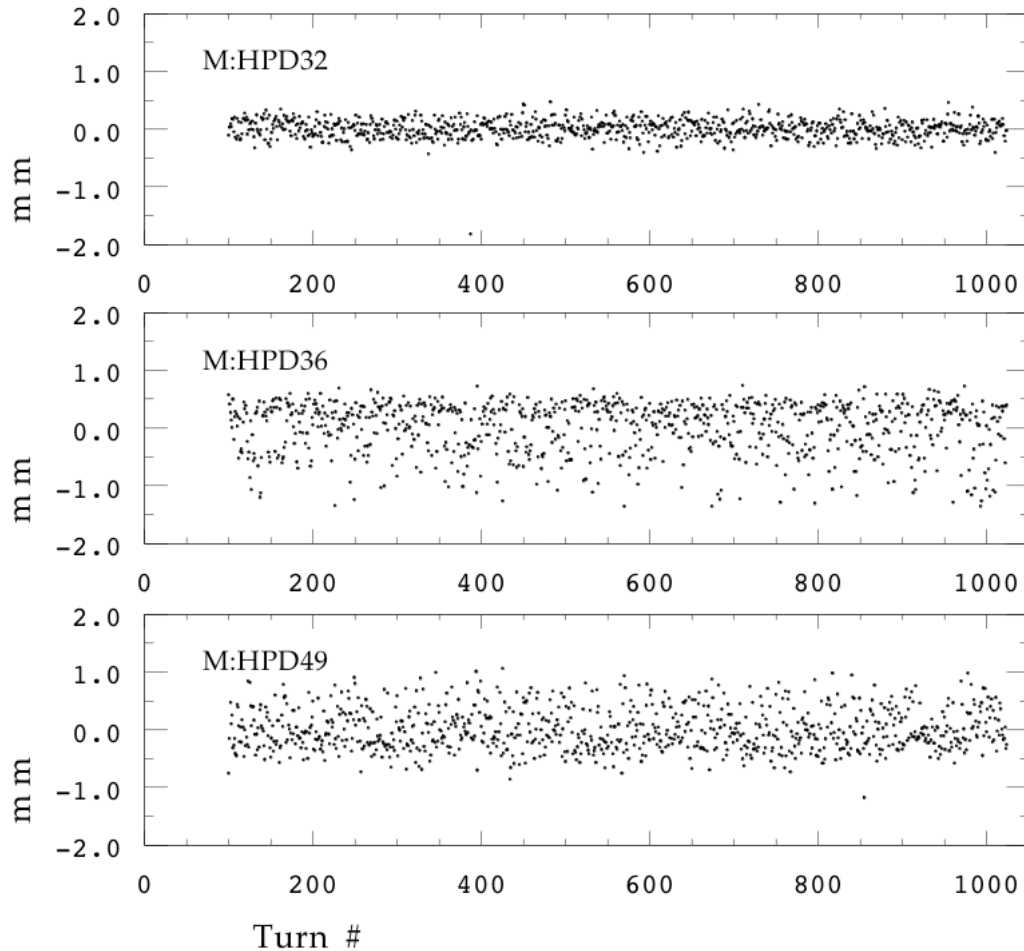


Figure 6. BPM deviation plotted against the turn number.

The emphasis here is that the error statistics may not uniquely point to the problem but will likely help in locating it. Because of the large number of turns,

up to 1024, this error information can have good statistical power. In general there is enough diagnostic information caused by problems like dead BPM signal, bad calibration, noisy, or even wrong polarity.

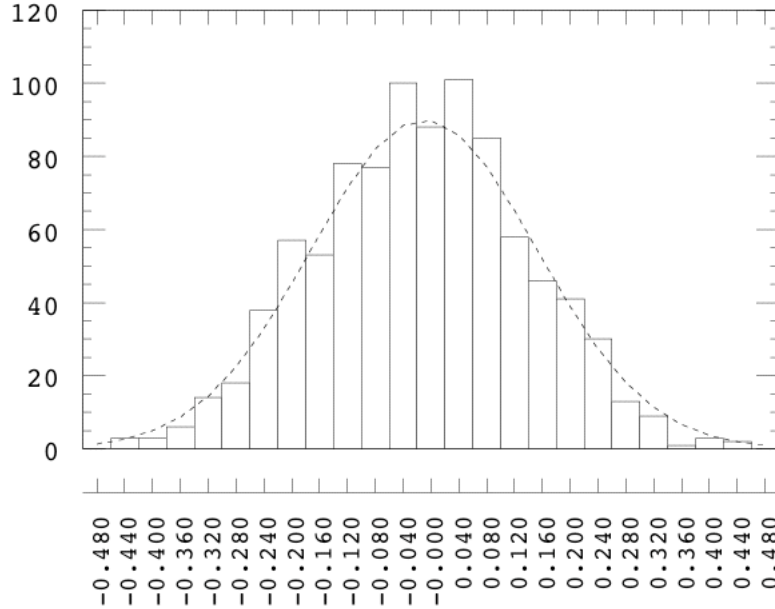


Figure 7. Histogram of BPM HPD32 deviation. The dotted line is a Gaussian curve using the estimated centroid and distribution sigma.

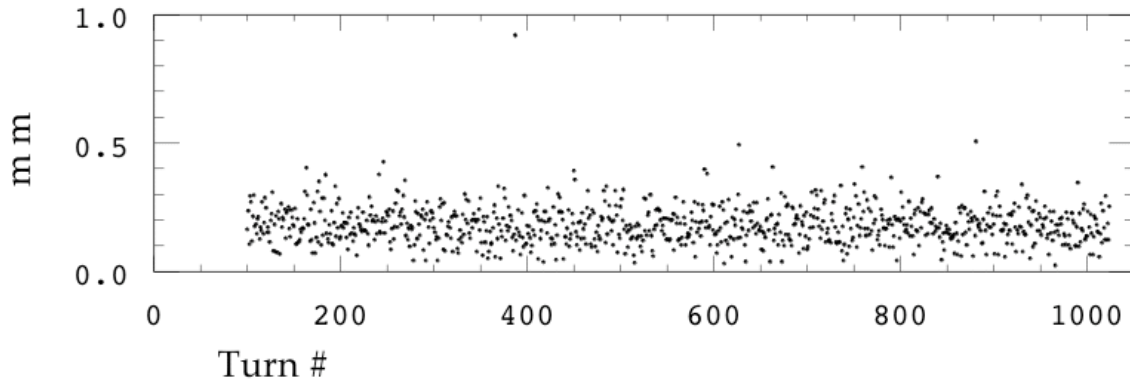


Figure 8. The refitted TBT RMS deviation from the same data as in Figure 4 but with HPD36 and HPD49 removed from the fitting analysis.

#### 4.2.3 TBT $\Delta p/p$

The beam energy error  $\Delta P/P$  is plotted in Figure 9, from the same data set used within this write-up. This type of error can be identified visually by looking at the TBT horizontal position. As one of the parameters in the fit to the horizontal plane BPM data it is also available numerically and can be used to correct beam position and angle due to  $\Delta P/P$  error. From the figure the synchrotron os-

cillation amplitude is almost visible beyond the noise level of the fitted data. Since each turn takes about  $21 \mu\text{sec}$  the oscillation is estimated to be about 90 Hz. The expected frequency from Main Ring beam at 150 GeV is about 70 Hz.

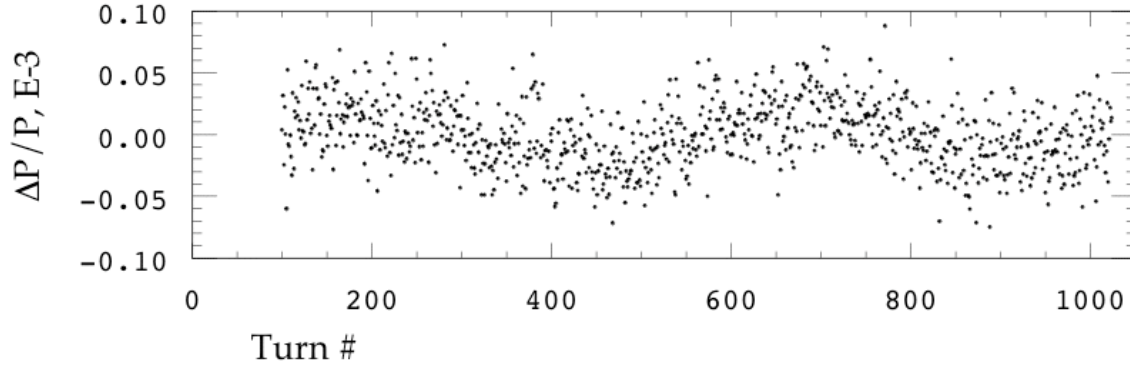


Figure 9. The  $\Delta P/P$  plot from fitting horizontal BPM data.

#### 4.2.4 Lattice verification

The transfer matrix used in the fitting of BPM data represents the knowledge about the beam line optics. Error in that knowledge leads to systematic error in the final result. The TBT data provides diagnostic abilities on this type of error. The level of sensitivity will depend on the resolution and noise level in the BPM data as will be discussed in the section on the simulated data.

### 4.3 FITTING THE PHASE SPACE ELLIPSE

There are five parameters needed to describe an ellipse. Among them two are used to specify the center of ellipse in the  $x-x'$  space. Another is used to specify the area of the ellipse, the emittance. Only two of them would have the information on the lattice function  $\alpha$  and  $\beta$ . To try to fit all five parameters would be a much more difficult task. The equations shown in section 2.4 applies only when the ellipse is centered at the origin of the phase space. To approximate this the center of ellipse is taken to be the average of all data points used and is subtracted off before proceeding with the fit. The validity of this approach is near perfect when the number of turns used gets beyond 50.

The result of fitting ellipse to phase space data points to get the area,  $\alpha$ , and  $\beta$ , the calculation of the tune, and the estimated error on the fitted values are given here.

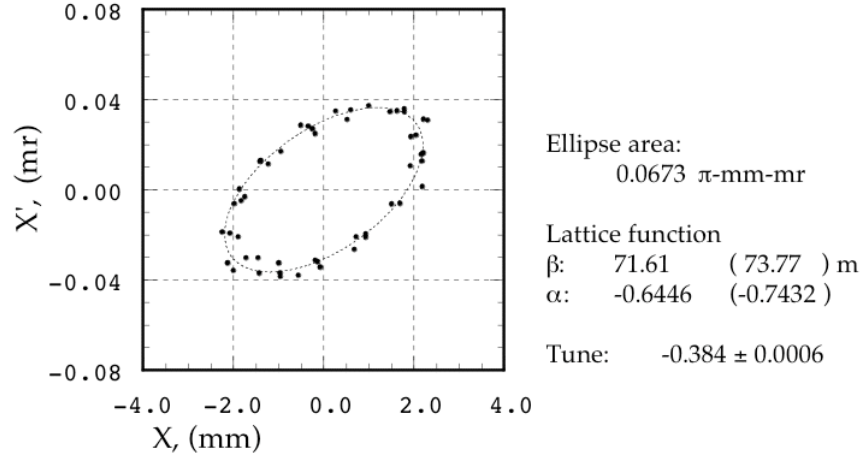


Figure 10. X and X' phase space plot for 50 consecutive turns. The fitted ellipse is shown in solid lines and the fitted values are shown to the right. The design lattice function is shown enclosed within the parenthesis.

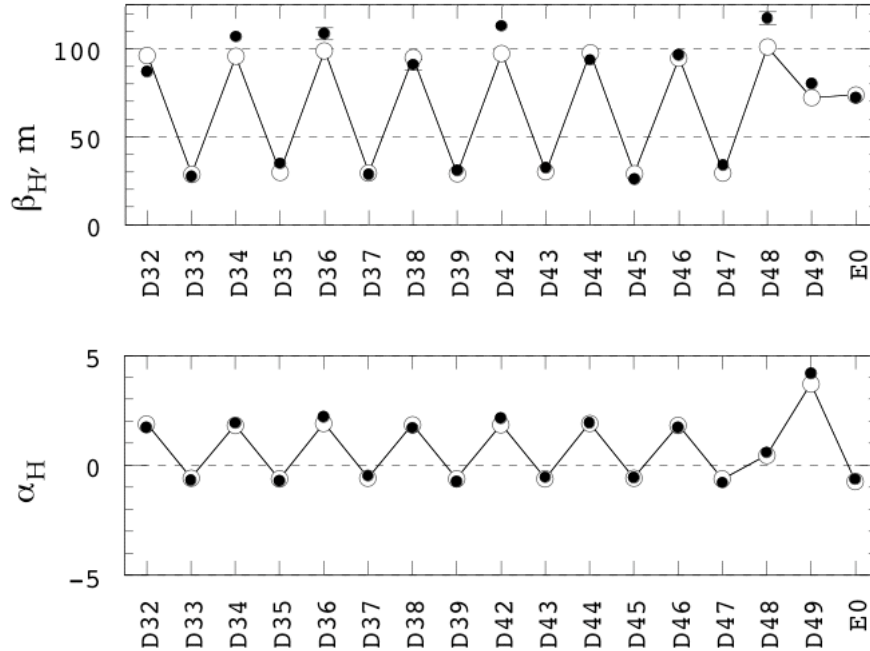


Figure 11. The lattice function at the BPM locations as derived from the data is shown in solid dots. The sigma of the distribution of the fitted beta is shown as error bars. The open circles with connecting lines are from the SYNCH calculation.

#### 4.3.1 Lattice function calculation

In Figure 10 is an example with 50 turns of phase space data at the Main Ring E0 straight location. The fitted ellipse is shown in dotted line. The fitted lattice function and the design lattice function are also displayed. The same calculation can be done to other BPM locations. Figure 11 plots the lattice function

at each BPM location as calculated from data and as designed. In (a) is the beta function and (b) the alpha function. The error bars are the estimated RMS of the distribution of the fitted lattice function and will be mentioned later.

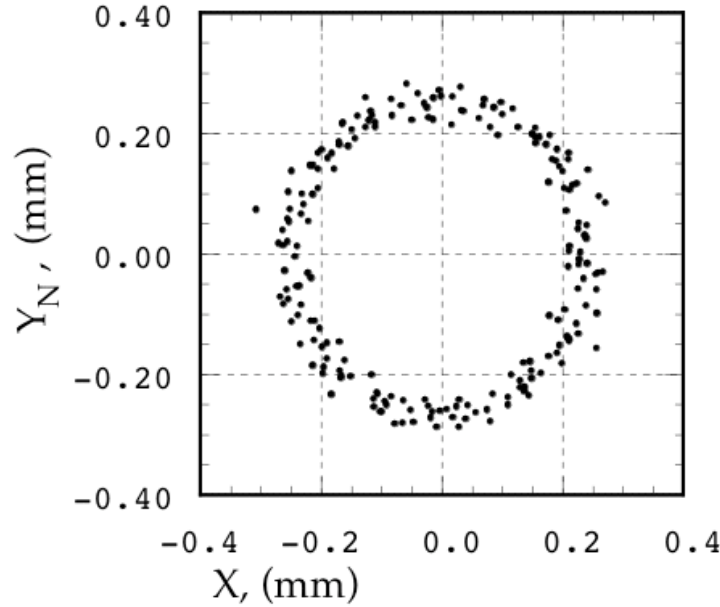


Figure 12. The normalized phase space plot. This is Figure 3 plotted in normalized phase space using fitted lattice function.

#### 4.3.2 Tune

Figure 12 shows the normalized phase space plot of the same data as used in Figure 3 using the fitted lattice function  $\alpha$  and  $\beta$  shown in Figure 10 and with the following transformation to the normalized phase space:

$$X = x$$

$$Y_N = \beta \cdot x' + \alpha \cdot x$$

The TBT tune as mentioned in equation 2-(9)&(10) is interesting in study the de-tuning effect due to higher order non-linear field. The tune information is extracted as shown in Figure 13. The solid dots are normalized phase space angles calculated with an accumulated offset to make the angle monotonically increasing. A linear fit to the angles with respect to the turn number gives the tune. The deviation from the linear fit is shown in open diamonds and ranges from -.03 to +.03, in unit of  $2\pi$ . Typically a tune measurement resolution of about 1 part in a thousand is possible with only 20 turns of data. The FFT method would require 1024 turns for the same accuracy.

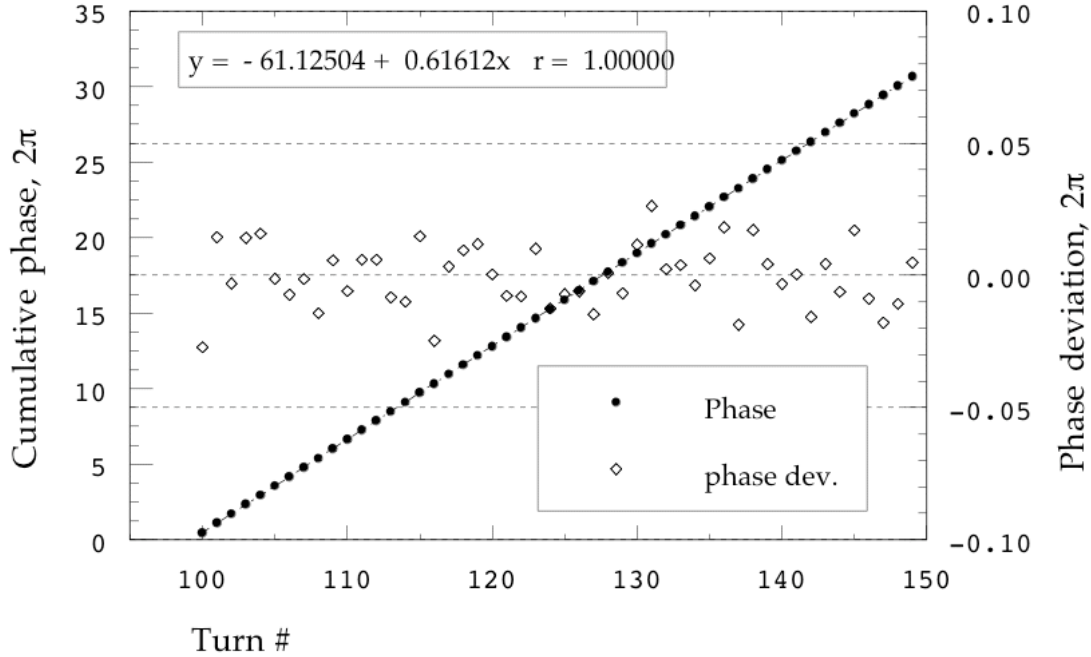


Figure 13. TBT tune calculation. The normalized phase space angles are plotted in solid dots with the vertical scale shown on the left hand side. The phase angle deviations are plotted in open diamonds with the vertical scale shown on the right.

#### 4.3.3 Error estimate

Because of the way ellipse is fitted an analytical error analysis is quite difficult with all the substitutions involved. Fortunately, because it takes only about 20 turn of TBT data to get a decent sample there is an empirical way of estimating the error. If  $n$  number of turns is chosen to do the fitting from a data set of  $N$  total consecutive turns there will be a set of  $(N - n + 1)$  possible sample. The variation among all possible sample can be used to estimate the error.

Usually it is a good idea to fit with enough points to get a better centroid averaged. On the other hand if the systematic effect is significant the number of turns used needs to be kept to a minimum.

##### 4.3.3.1 Statistical

The BPM data is subjected to error due to noise on the BPM signal and the digitization resolution. This will cause error in the calculated phase space points and consequently the fitted lattice function. This type of errors are un-correlated and will be statistical in nature. Figure 14 shows the histogram of the fitted beta function with each sample using 30 turns of data. The sigma of the histogram simply states the extend of variation in the fitted result as was done in Figure 11,

which plots the average and distribution sigma at all the BPM locations. If there is no systematic effect the centroid and width of the histogram will be the statistical resolution.

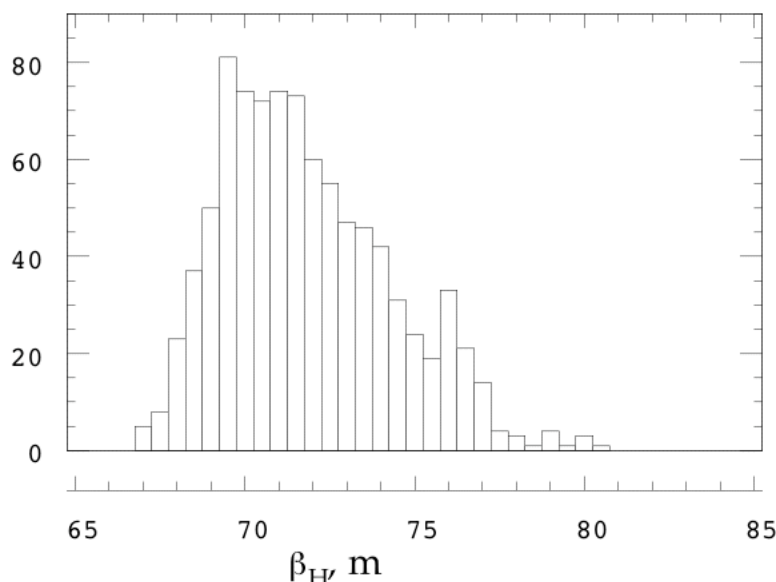


Figure 14. Histogram of fitted beta function at EØ. The sample window is set at 30 turns.

#### 4.3.3.2 Systematic

In reality the systematic effect always clouds the picture. The systematic error is very crucial in this type of lattice function calculation. Constant attention to the goodness of fit at every stage is advised.

##### *Lattice model used*

If the transfer matrix is from a wrong lattice model the calculation for the phase space point can be wrong. There will still be a phase space distribution that looks like an ellipse. This will result in a slightly different value for the lattice function. If the error is caused by unsteady magnet current the error will change in time as well.

##### *Bad TBT data*

Bad data can be a result of many things going wrong. For example, the BPM data could have a wrong sign, a bad calibration, a time dependent drift in signals from electronics, or could simply be dead. Problem of this sort usually leads to poor beam parameter fitting statistics. The data can also be corrupted

such that the BPM data used to fit for beam parameter does not all come from the same turn number.

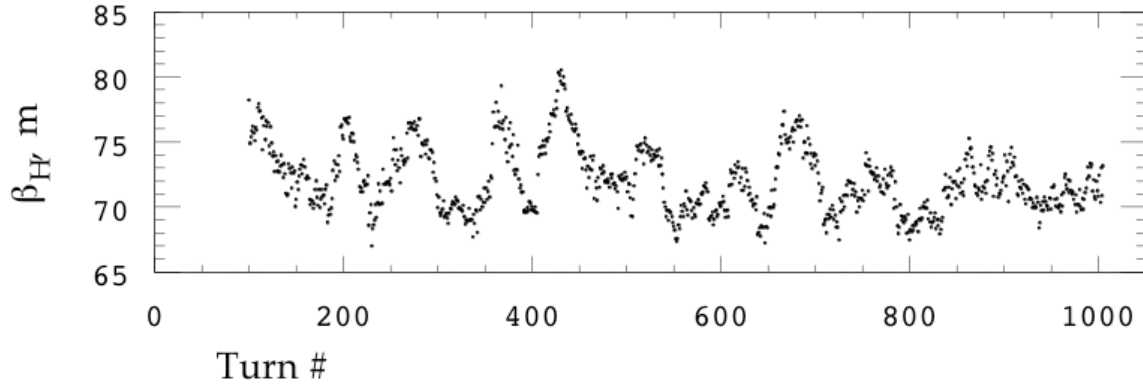


Figure 15. The fitted beta plotted against the turn number.

#### *Data stability*

Typically using more turns to fit for lattice function should in principle give an averaging effect. However, systematic effects caused by the electronics, the x-y plane coupling, or the orbit drift due to magnet current can distort the phase space population asymmetrically and cause bias to the fitted lattice function.

Figure 15 takes the same result used in Figure 14 and plots them with respect to the turn number. The fitted beta function appears to be changing in time. There could be more than one possible cause and it needs to be examined carefully.



## 5. Simulation

The purpose of doing simulated data is to evaluate the systematic effects caused by an error condition, to identify the signature of an error condition, and to answer the question of whether a fit is good enough for the given data accuracy. Typically there are three major issues that the simulation can explore. The first is the noise problem which includes the ADC resolution. The second is the accuracy of transfer matrix being used to analyze data. The third is about the coupling. The study of the effect of coupling has on the lattice function measurement is not finished and will not be covered in this write-up.

In addition to generating ideal data the simulation also packages data into exactly the same data buffer format as in the actual data. The simulated data then gets processed through exactly the same way as the real data to reduce possible differential treatment of different type of data.

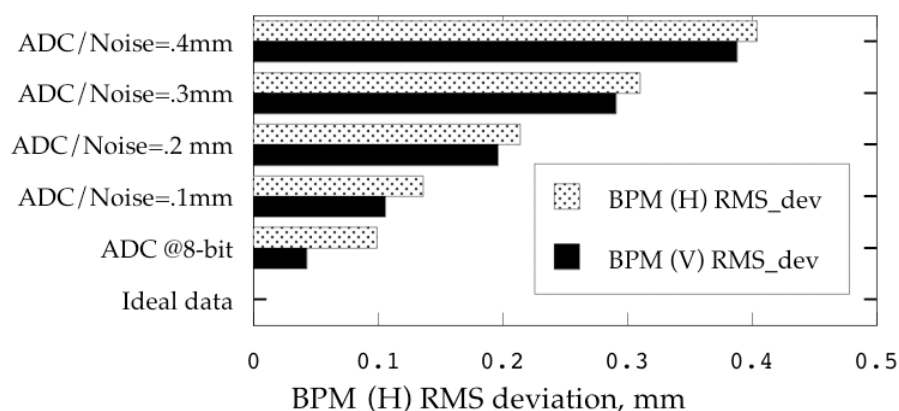


Figure 16. BPM position deviation using simulated data. All the data shown have the effect of a 8-bit ADC included except for the ideal data.

### 5.1 NOISE AND DATA RESOLUTION

The BPM hardware gives the position in an 8-bit data covering both polarity. The data is then re-scaled using a pre-calculated lookup table. To simulate the effect of digitization the routine calculates the expected beam positions and references the lookup table to produce an 8-bit data. The noise level can be set to zero, to a certain level, or to that derived from fitting the actual data. This way one can estimate how much of the fitted lattice function is affected by the noise. Figure 16 shows TBT RMS deviation from the fit to simulated BPM position data at varying data accuracy. The ideal data, which has infinite ADC resolution and

no noise, has essentially zero RMS deviation. For Fermilab Main Ring, the position resolution due to the 8-bit ADC is about .3 mm horizontally and .12 mm vertically. The effect of the ADC resolution is reflected in the data set marked "ADC@8-bit". All others have both the ADC resolution and noise effect. As a comparison the real data shown in Figure 4 has a averaged TBT RMS of around .25 mm.

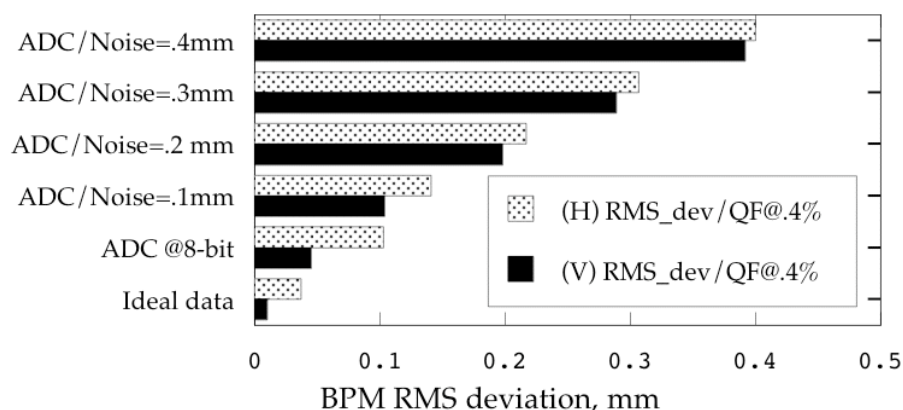


Figure 17. The BPM position deviation with simulation error. Same as in the Figure 16 but the transfer matrix used to generate data is slightly different from the one used for analysis. The strength of the horizontal focusing quad bus current, QF, was set to be .4% higher while generating the simulation data.

## 5.2 TRANSFER MATRIX

The simulation program uses a separate set of transfer matrix, which may or may not be the same as the one used by the analysis program, to generate Monte Carlo data. It is possible to study the errors caused by using incorrect transfer matrix.

Figure 17 shows the effect of transfer matrix error and is to be compared with Figure 16. The only appreciable difference between the two figures is in the data set called "Ideal data". The horizontal RMS is much larger because the error is on the focusing quads where vertical beta function is small. This effect, however, is not quite visible after the ADC resolution is included in the simulation. This demonstrated the level of sensitivity the current BPM system have on the transfer matrix error, based on the BPM positions along.

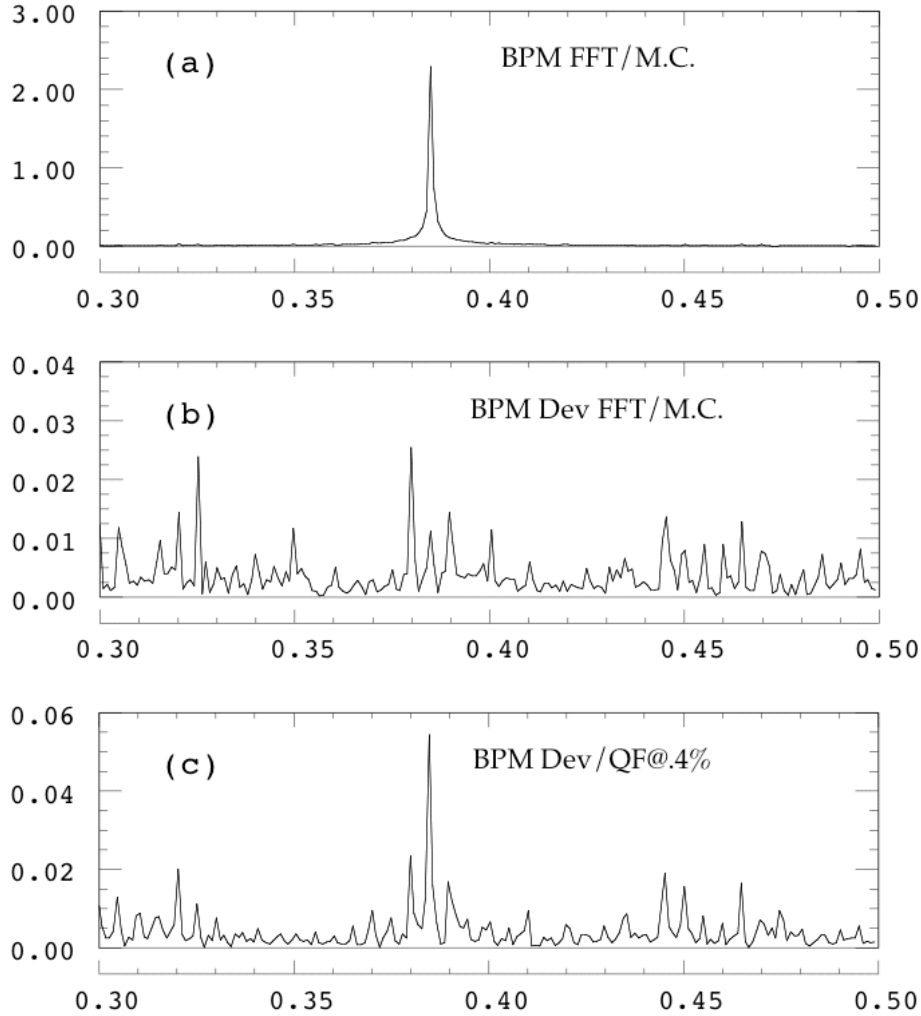


Figure 18, FFT spectrum from the simulated data.

As was mentioned earlier there is a lot of statistical power in the TBT data. In Figure 18(a) is a FFT spectrum of BPM position which shows the fractional tune of the horizontal betatron oscillation. Figure 18(b) shows the FFT spectrum of BPM position deviation from the fit. As was expected, there is no visible betatron frequency in the spectrum. Figure 18(c) is a similar display as in 18(b) except that the transfer matrix used to generate the data has a focusing quad bus current error of +.4%. There is definitely a hint of betatron frequency in the spectrum. Turn our attention to the FFT spectrum from the real data used in this write-up and shown in Figure 19. In (a) is the BPM position FFT spectrum and (b) the BPM position deviation FFT spectrum. Again there is visible betatron frequency. The higher background level could be attributed to the fact that the betatron oscillation was induced at around the 90-th turn in the real data. The transfer matrix error is likely not the only one that could contribute to this effect.

But if indeed such error exist the BPM system would be sensitive to the level of .4% in bus current.

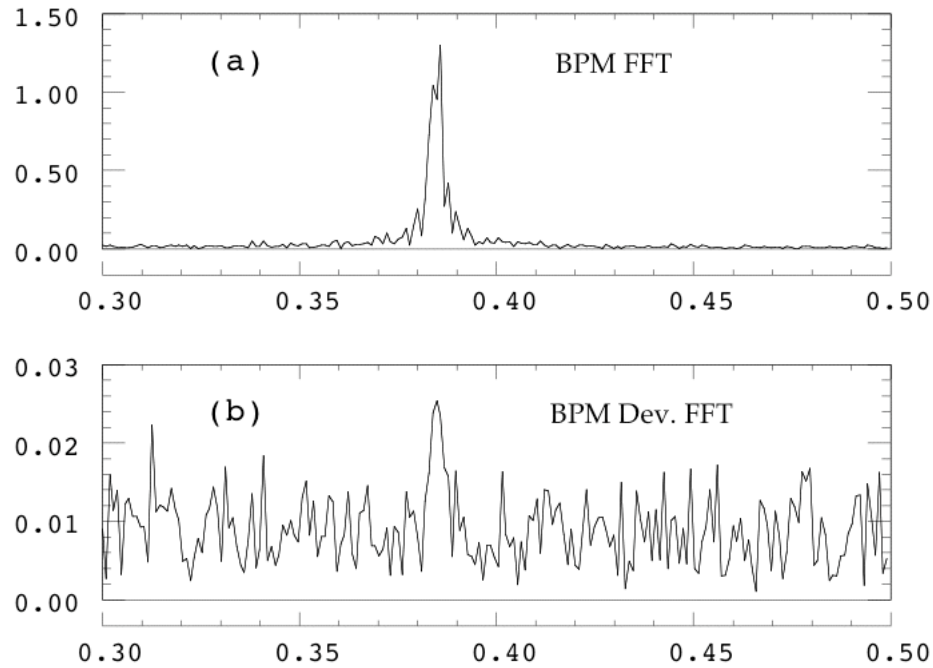


Figure 19. The FFT spectrum from actual data set used within this write-up.

### 5.3 LATTICE FUNCTION ERROR

The algorithm used to fit the ellipse at present does only straight fitting and is likely to have bias depending on the data set. By using simulation data many of the biases can be evaluated and in some cases eliminated. Figure 20 and

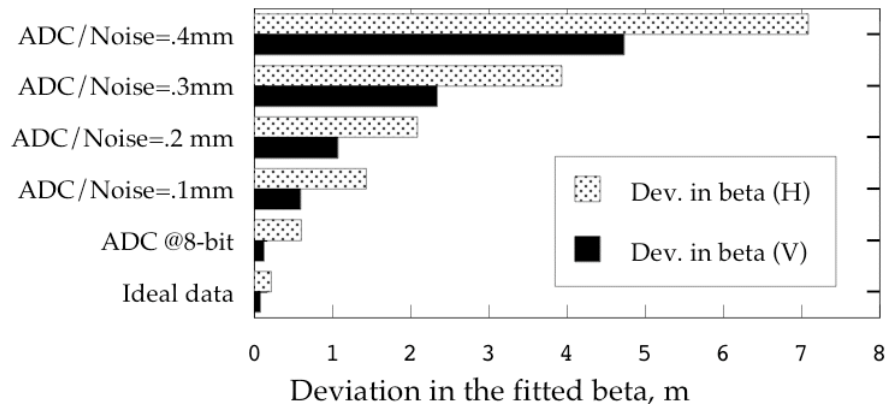


Figure 20. The deviation RMS of fitted beta value from the beta used due to ADC resolution and noise.

21 show one example where the simulation is used to evaluate the effect of noise and ADC resolution on the fitted lattice function beta and the distribution RMS.

There appears to be substantial bias on the beta function as the noise level increases. The earlier assessment puts the BPM data noise level some where between .2 and .3 mm and consequently a possible bias of about 3 meters in beta function. Similar data can be obtained for the alpha function but is not shown in this write-up.

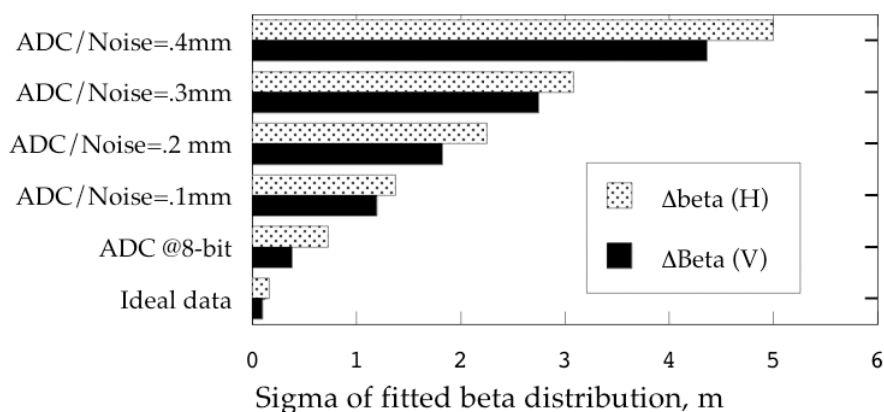


Figure 21. The RMS of fitted beta value distribution due to ADC resolution and noise.

## 6. Conclusion

Knowing the lattice function is important for matching lattice functions between two different machines during beam transfer and for understanding of the machine as well. The technique introduced in this write-up gives both the  $\beta$  and  $\alpha$  value needed for a complete matching. Since the phase space area of the ellipse is a fitted parameter it is not sensitive to how the betatron oscillation is introduced. In the near future the BPM system will be upgrade to provide data on every BPM available. The potential for measuring the lattice function around the whole ring is very real. With future improvement to the analysis software to reduce the systematic effect the TBT BPM data could very well be the ideal instrument to machine lattice measurement.

This write-up is intended to give a clear picture of what is being done to extract the lattice function from data available in the Fermilab BPM system. The procedure is very quick once the machine is setup to take data. The data it produces is reproducible but is also very susceptible to systematic effect. The validity of the result can only be ensured if one takes great care to maintain the integrity of data, to use the correct transfer matrix, and to pay attention to the diagnostic information.

- 
- [1] Glen Goderre, Beta function measurement at Fermilab Tevatron.
  - [2] K. Steffen, p. 43, CERN Accelerator School 85-19
  - [3] Fermilab Operation Bulletin #888.